Detecting and characterizing downed dead wood using terrestrial laser scanning

Yrttimaa, Tuomas

2019-05

Yrttimaa , T , Saarinen , N , Luoma , V , Tanhuanpaa , T , Kankare , V , Liang , X , Hyyppa , J , Holopainen , M & Vastaranta , M 2019 , ' Detecting and characterizing downed dead wood using terrestrial laser scanning ' , ISPRS Journal of Photogrammetry and Remote Sensing , vol. 151 , pp. 76-90 . https://doi.org/10.1016/j.isprsjprs.2019.03.007

http://hdl.handle.net/10138/328024
https://doi.org/10.1016/j.isprsjprs.2019.03.007

Detecting and characterizing downed dead wood using terrestrial laser scanning

Tuomas Yrttimaa[a,b*], Ninni Saarinen[b,a], Ville Luoma[b], Topi Tanhuanpää[b,c], Ville Kankare[a,b], Xinlian Liang[d], Juha Hyyppä[d], Markus Holopainen[b], Mikko Vastaranta[a]

[a] School of Forest Sciences, University of Eastern Finland, P.O. Box 111, 80101 Joensuu Finland; tuomas.yrttimaa@uef.fi, ville.kankare@uef.fi, mikko.vastaranta@uef.fi.

[b] Department of Forest Sciences, University of Helsinki, P.O. Box 27, 00014 University of Helsinki, Finland; ninni.saarinen@helsinki.fi, ville.luoma@helsinki.fi, markus.holopainen@helsinki.fi.

[c] Department of Geographical and Historical Studies, University of Eastern Finland, P.O. Box 111, 80101 Joensuu, Finland; topi.tanhuanpaa@uef.fi.

[d] Department of Remote Sensing and Photogrammetry, Finnish Geospatial Research Institute (National Land Survey of Finland), Geodeetinrinne 2, 02431 Masala, Finland; xinlian.liang@nls.fi, juha.hyyppa@nls.fi.

[*] Corresponding author; email tuomas.yrttimaa@uef.fi

Pre-print of published version.
Reference:
Yrttimaa, T., Saarinen, N., Luoma, V., Tanhuanpää, T., Kankare, V., Liang, X., Hyyppä, J., Holopainen, M., Vastaranta, M. 2019. Detecting and characterizing downed dead wood using terrestrial laser scanning. ISPRS Journal of Photogrammetry and Remote Sensing (151), pp. 76–90.

DOI:
https://doi.org/10.1016/j.isprsjprs.2019.03.007

Abstract

Dead wood is a key forest structural component for maintaining biodiversity and storing carbon. Despite its important role in a forest ecosystem, quantifying dead wood alongside standing trees has often neglected when investigating the feasibility of terrestrial laser scanning (TLS) in forest inventories. The objective of this study was therefore to develop an automatic method for detecting and characterizing downed dead wood with a diameter exceeding 5 cm using multi-scan TLS data. The developed four-stage algorithm included 1) RANSAC-cylinder filtering, 2) point cloud rasterization, 3) raster image segmentation, and 4) dead wood trunk positioning. For each detected trunk, geometry-related quality attributes such as dimensions and volume were automatically determined from the point cloud. For method development and validation, reference data were collected from 20 sample plots representing diverse southern boreal forest conditions. Using the developed method, the downed dead wood trunks were detected with an overall completeness of 33% and correctness of 76%. Up to 92% of the downed dead wood volume were detected at plot level with mean value of 68%. We were able to improve the detection accuracy of individual trunks with visual interpretation of the point cloud, in which case the overall completeness was increased to 72% with

mean proportion of detected dead wood volume of 83%. Downed dead wood volume was automatically estimated with an RMSE of 15.0 m^3/ha (59.3%), which was reduced to 6,4 m^3/ha (25.3%) as visual interpretation was utilized to aid the trunk detection. The reliability of TLS-based dead wood mapping was found to increase as the dimensions of dead wood trunks increased. Dense vegetation caused occlusion and reduced the trunk detection accuracy. Therefore, when collecting the data, attention must be paid to the point cloud quality. Nevertheless, the results of this study strengthen the feasibility of TLS-based approaches in mapping biodiversity indicators by demonstrating an improved performance in quantifying ecologically most valuable downed dead wood in diverse forest conditions.

Keywords: TLS, biodiversity, point cloud, coarse woody debris, CWD, ground-based LiDAR

1. INTRODUCTION

Dead wood, or coarse woody debris (CWD), including standing and downed dead trees, woody debris, and stumps, is an important structural component in boreal forest ecosystems as it maintains the forest biodiversity and stores carbon decades after the tree death has occurred (Franklin et al. 1987; Krankina, Harmon 1995; Harmon, Sexton 1996; Esseen et al. 1997). The abundance of CWD is considered to be an indicator of forest biodiversity, since many threatened species are dependent on decaying wood as a habitat (Harmon et al. 1986; Esseen et al. 1997; Siitonen 2001). Most often, these species are specialized in CWD with certain properties (i.e., tree species, stage of decay, water content, size and orientation) (Jonsell, Weslien 2003; Similä et al. 2003; Tikkanen et al. 2006). Being a dynamic pool for carbon, CWD has a major role in the circulation of carbon and nutrients (Harmon et al. 1986; Franklin et al. 1987; Russell et al. 2015). The proportion of carbon stored in CWD in a forest can be substantial depending on the disturbance history and the maturity of the forest (Krankina, Harmon 1995). When assessing carbon stores and fluxes in a forest ecosystem, it is essential to also include carbon stored in CWD. This requires quantifying the CWD which has traditionally based on field inventory (see Russell et al. 2015). Complementary approaches for CWD mapping using optical remote sensing (e.g., Bütler, Schlapfer 2004; Pasher, King 2009) as well as airborne laser scanning (ALS) (Pesonen et al. 2008; Lindberg et al. 2013; Nyström et al. 2014; Tanhuanpää et al. 2015) have been introduced. Still, field inventory with traditional forest mensuration tools have been required when detailed information on dead wood dynamics is needed.

During the last decade, the high potential of terrestrial laser scanning (TLS) in acquiring dense point clouds for characterizing forest structure has been noticed (Dassot et al. 2011; Newnham et al. 2015; Liang et al. 2016; Liang et al. 2018). TLS provides a detailed three-dimensional description of the surroundings of the scanner enabling versatile measurements from single trees and tree communities with a millimetre-level of detail. Developments in scanner technology, as well as advances in computational performance and data storing capacity have awoken the growing interest for the use of TLS-based approaches in forest inventory applications (Liang et al. 2016; White et al. 2016). Previous studies have proven TLS-based methods to be feasible for detecting most of the trees as well as providing information on tree attributes, such as tree height and diameter at breast height (DBH) (e.g. Maas et al. 2008; Liang, Hyyppä 2013; Heinzel, Huber 2016; Korén et al. 2017; Cabo et al. 2018). A major advantage of TLS is the ability to non-destructively estimate some of the important tree attributes (e.g., stem curve and volume) that have been challenging to be determined accurately using the conventional field inventory methods (Liang et al. 2014a; Olofsson, Holmgren 2016; Sun et al. 2016; Saarinen et al. 2017). In addition, tree biomass can be modelled with improved accuracy as the stem and large part of the branches can be measured from the TLS data (Kankare et al. 2013; Seidel et al. 2013; Ishak et al. 2015; Calders et al. 2015; Stovall et al. 2017). To emphasize the versatility of the use of TLS in forest applications, TLS has also been used in analysing timber quality (Kankare et al. 2014; Pyörälä et al. 2018) and canopy structure (e.g. Henning, Radtke 2006; Fleck et al. 2007;

Danson et al. 2014). State-of-the-art methodologies in detecting and characterizing trees using TLS data were recently investigated in an international benchmarking study, in which 18 different algorithms were compared in varying southern boreal forest conditions (Liang et al. 2018). The study revealed that challenges still exist, especially in tree detection and tree height estimation. The use of TLS in sample plot measurements is also restricted due to the lack of methods for automatic tree species recognition, which has been investigated less frequently (Liang et al. 2016; Åkerblom et al. 2017).

The main driver in developing new TLS-based methods has been the utilization of point clouds to complement or even replace the conventional field inventory methods. The experience gained from the past studies, the international benchmarking by Liang et al. (2018), as well as the discussion on the best practices in TLS data acquisition by Wilkes et al. (2017), for example, have been significant milestones towards operational applicability of TLS-based methods. In addition to attributes of standing trees, TLS technology should be suitable for characterizing the forests through topography, low vegetation and downed trees as well. However, the priority in studies regarding the use of TLS for forest characterization has been the retrieval of the attributes of the living standing trees, while less effort has been put in detecting other ecologically valuable structures, such as CWD (see Marchi et al. 2018). Polewski et al. (2017), on the other hand, recently introduced the first attempt to map downed trees automatically from TLS point clouds by applying a statistical cylinder detection framework. According to Polewski et al. (2017), it seems that the use of TLS-based approach in mapping downed trees is feasible at least in relatively sparse forests with fallen trees large in diameter. Putman and Popescu (2018) estimated the volume of standing dead trees using TLS data but, as stated in Polewski et al. (2017), the conditions for tree detection and presumably also for diameter measurement, for example, are more challenging for downed trees than for standing trees. Thus, a knowledge gap regarding the feasibility of TLS-based approaches to provide information on dead wood quality attributes such as dimensions still exists and currently limits the use of TLS for comprehensive characterization of forests.

The objective of this study was to develop a method for detecting and characterizing downed dead wood using point clouds from multi-scan TLS data. In this study, downed dead wood is defined as stems or part of the stems that have fallen on the forest floor because of natural disturbance or harvesting, hereafter denoted as downed dead wood or dead wood trunks. In the developed method, the dead wood trunks are detected based on their geometric properties. The dead wood trunks are delineated from the point clouds for measuring trunk dimensions and for deriving the quantity and quality of downed dead wood on a sample plot. The quantity of dead wood is measured as the total volume of dead wood and the number of dead wood trunks on a sample plot. Dead wood quality is described through attributes related to the trunk dimensions that are expected to be measurable from TLS point clouds. The performance of the TLS-based approach is examined on 20 sample plots representing diverse southern boreal forest conditions. The study aims to strengthen the feasibility of TLS-based approach in dead wood mapping expanding the applicability of dense point clouds in forest inventories.

2. MATERIALS AND METHODS

2.1 Study materials

2.1.1 Study area

The study area is located in Evo, southern Finland (Figure 1), where the forests are dominated by Scots pine (*Pinus sylvestris* L.), Norway spruce (*Picea abies* (L.) H. Karst.) and birch (*Betula L.* sp). The forests in the area are characterized by a mixture of managed and natural forests including both homogeneous and heterogeneous stands with varying growth stages.

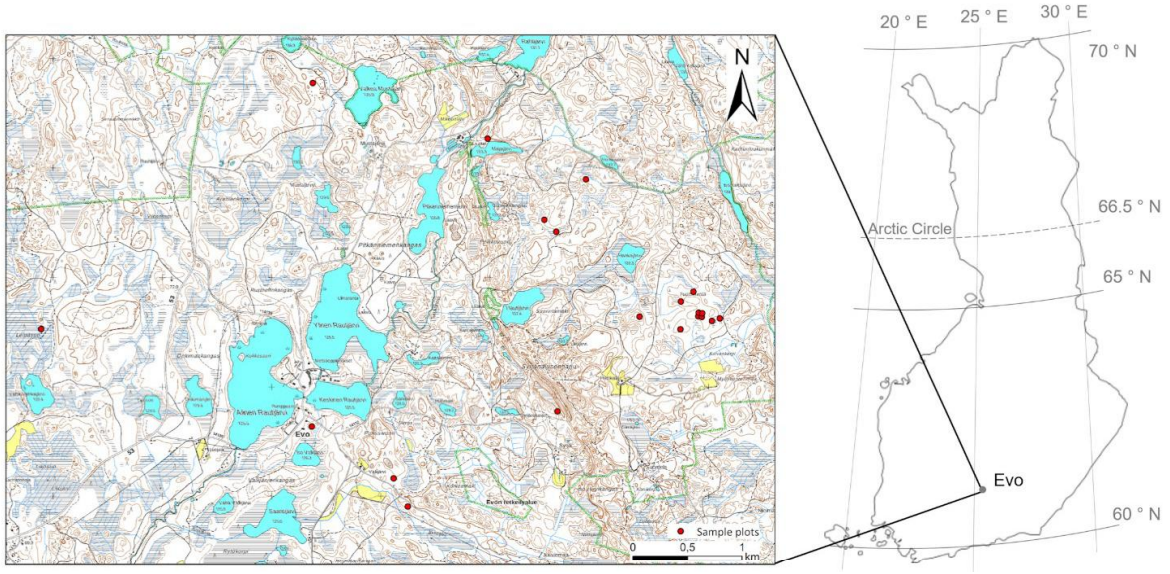

Figure 1. Map of the study area and the locations of the sample plots.

2.1.2 Sample plot characteristics

The method development in this study was based on TLS data collected from 20 sample plots (32 m x 32 m in size) in autumn 2017. The sample plots were selected from a group of 91 sample plots which were established in 2014 to cover the structural variation of forests in the study area (for more details, see Yu et al. 2015). TLS data were available from these sample plots enabling virtual revisit to the study site for assessing the abundance of downed dead wood which was the main criterion determining the sample plot selection. Standing trees on the sample plots with a DBH exceeding 5 cm had been measured in the field in summer 2014. Tree species, DBH, height, stem volume and location had been determined for each tree. DBH was measured with steel callipers, and height was derived using electronic clinometer. DBH and height were then used to estimate the stem volume with species-specific volume equations (Laasasenaho 1982). Location of each tree was derived by either detecting the tree from the TLS point cloud or by determining the location in the field with respect to the known locations of the detected trees. Finally, stand attributes describing the forest structure at stand-level were calculated based on individual tree attributes.

The sample plots were located in both managed and natural forests with Lorey's mean height, basal-area weighted mean diameter, basal area, volume, and stem number varying between 18.7–31.3 m, 19.0–42.7 cm, 15.2–42.9 m^2/ha, 177.7–507.7 m^3/ha, and 324–2041 n/ha, respectively (Table 1). For each sample plot, dominant tree species was defined by the species with largest basal area. Norway spruce was the dominant tree species for 16 sample plots, Scots pine for two sample plots, Downy birch (*Betula pubescens* L.) for one sample plot, and Siberian larch (*Larix sibirica* Ldb.) for one sample plot.

Table 1. Variation of forest structural attributes on the sample plots (n = 20) used for method development. Dg = basal area weighted mean diameter, Hg = Lorey's mean height, G = basal area, V = stem volume, S = stem density, based on field measurements in summer 2014.

	Dg (cm)	Hg (m)	G (m^2/ha)	V (m^3/ha)	S (n/ha)
min	19.0	18.7	15.2	177.7	342
mean	31.6	25.0	29.9	341.7	728
max	42.7	31.3	42.9	507.7	2041
standard deviation	7.4	4.1	6.9	102.9	392

2.1.3 Terrestrial laser scanning data acquisition

TLS data were collected in leaf-off conditions in early November 2017, using Leica HDS6000 phase-shift scanner (Leica Geosystems, Heerbrugg, Switzerland). The scanning was conducted with high power setting, providing a point cloud with point spacing of 6.3 mm and point density of approximately 25 000 points/m^2 at 10 m distance from the scanner. The data were collected using a multi-scan approach with five scanning positions for each plot. The first scanning position was located at the plot centre, while the remaining four scanning positions were placed around the first one in quadrant directions in order to cover the entire plot. The point clouds were then registered and combined using spherical reference targets attached to the trees with steel plates and magnets. Depending on the vegetation density, the number of reference targets used for point cloud registration was from five to six targets per plot. All the reference targets were visible from the plot centre, and at least three of them from all other scanning positions. In this way, the point clouds from each scanning location could be combined. The exact location of each reference target was measured using a total station and ground control points. The locations were used in transforming the combined point clouds into global coordinate system.

TLS data acquisition was followed by point cloud registration and filtering. The registration was conducted using Z + F LaserControl software (Zoller + Fröhlich GmbH, Wangen im Allgäu, Germany). First, the reference targets were visually detected and identified from the point cloud. Then, spherical objects of equal size to the reference targets were fitted to the points representing the reference targets. Using the fitted spherical objects, 3D-transformation between the point clouds (i.e., point cloud rotation and translation with respect to the centre plot scan) were calculated. As a result, the point clouds could be combined at plot-level with a mean accuracy of 1.7 mm. In addition, mixed pixels (i.e., points that occur when the laser beam intersects two surfaces within a certain distance apart, resulting an inaccurate range measurement) were filtered to remove noise from the point cloud. Depending on the forest structure, the number of points in a point cloud representing an entire sample plot varied between 104 million to 150 million.

2.1.4 Reference measurements on downed dead wood

Quantity and quality of downed dead wood was measured in the field using steel callipers and a measuring tape to assess the accuracy of the TLS-based method for detecting dead wood. All downed dead wood trunks with a diameter exceeding 5 cm at the middle of the trunk were measured in the field and included in the field reference. For each trunk, tree species, bark coverage and stage of decay were determined based on field instructions for Finnish National Forest Inventory (Finnish Forest Research Institute 2009). The trunk was classified into five bark cover percentage classes based on ocular estimation. The stage of decay was determined based on how much the blade of a knife penetrated the wood: the depth of the penetration indicated how far the decay had proceeded. Additionally, dimensions of the trunk were measured using a measuring tape and steel callipers. The length and diameters were measured for each trunk. The diameters were measured at the butt-end, the top-end, and from the middle of the trunk, as well as at two-meter intervals, beginning from the butt-end of the trunk (Figure 2). Diameter in the middle of the trunk, i.e., the mid-diameter, was also considered as one of the attributes defining the quality of dead wood. Trunk dimensions were then utilized to estimate the trunk volume. The volume was calculated using the Huber formula (Equation 1) by dividing the trunk in sections and summing up the volume estimates of the trunk sections:

$$V = \sum_{i=1}^{n} A_{m_i} l_i = \sum_{i=1}^{n} \frac{\pi l_i}{16} (d_i + d_{i+1})^2 \quad (1)$$

where A_{m_i} is the cross-sectional area measured in the middle of the i^{th} trunk section, l_i is the length of i^{th} trunk section, n is the total number of trunk sections, d_i is the diameter measured at the butt-end and d_{i+1} diameter measured at the top-end of i^{th} trunk section. Each field-measured dead wood trunk was numbered, and the location and orientation of the trunk were marked into the tree map with respect to the standing trees on the sample plot.

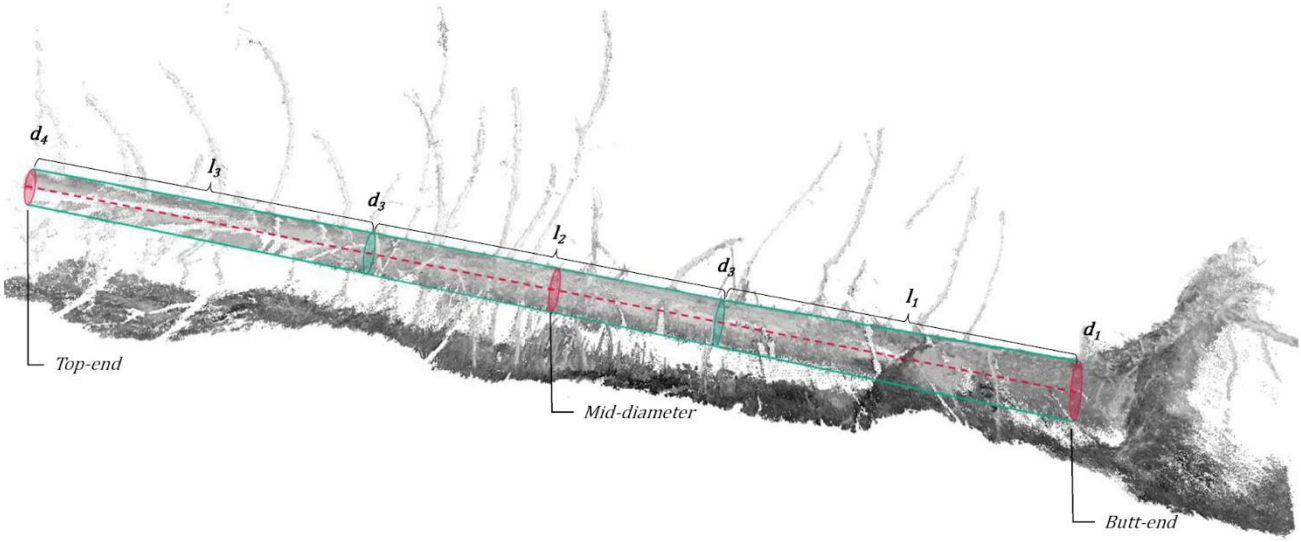

Figure 2. Illustration of a downed dead wood trunk delineated from the point cloud, and the dimensions measured in the field to derive the trunk volume (see Equation 1).

According to the reference measurements, the total volume of downed dead wood on sample plots varied from 2.8 to 61.4 m^3/ha (Table 2). Highest volumes occurred on sample plots in old unmanaged forests, while the lowest amounts of downed dead wood were observed in managed forests. Altogether, 304 dead wood trunks were measured in the field. Two thirds of the trunks were Norway spruces, while birches and Scots pines accounted for 19% and 10% of the trunks, respectively. Descriptive statistics on the field-measured downed dead wood trunk attributes as well as diameter distribution of the trunks are presented in detail in Table 3.

Table 2. Quality and quantity of downed dead wood on the sample plots. V = the dead wood volume, S = the number of measured dead wood trunks, decay-ratio = the ratio between the total volume of downed dead wood and the total volume of standing trees on a sample plot, d_m = the mean trunk mid-diameter, l_m = the mean trunk length, v_m = the mean trunk volume.

	V (m^3/ha)	S (n/ha)	decay-ratio (%)	d_m (cm)	l_m (m)	v_m (dm^3)
min	2.8	49	1.0	6.9	3.3	10.7
mean	25.3	150	7.4	14.3	7.6	192.6
max	61.4	479	25.3	21.0	11.6	460.3
standard deviation	18.6	97	5.8	3.8	2.2	127.8

Table 3. Descriptive statistics on the field-measured downed dead wood trunks (n = 304). Mid-diameter stands for the diameter measured from the middle of the trunk.

		mid-diameter (cm)		length (m)		volume (dm^3)	
min		5.0		0.9		3.4	
mean		13.3		7.2		170.5	
median		10.5		5.9		48.7	
max		39.5		28.0		2550.0	
standard deviation		7.7		5.4		316.8	
mid-diameter class (cm)	5–10	10–15	15–20	20–25	25–30	30–35	35–40
n	142	71	33	29	13	12	4
proportion of trunks (%)	46.7	23.4	10.9	9.5	4.3	3.9	1.3
proportion of volume (%)	7.0	13.1	12.5	24.7	17.2	21.7	3.8

2.2 Method for detecting and characterizing downed dead wood using TLS point cloud

2.2.1 TLS point cloud pre-processing

A TLS-based method for mapping downed dead wood from sample plots was developed using MATLAB (The MathWorks Inc, Natick, Massachusetts, United States). To be able to detect the dead wood trunks lying on the forest floor, the TLS point clouds were normalized. The height normalization was based on a digital terrain model (DTM) generated from the TLS point clouds.

The initial group of points were generated by dividing the point cloud into 0.5 m x 0.5 m grid on the xy-plane and searching for the lowest value for z-coordinate among the points in each grid cell. The points whose mean distance to the four neighbours was larger than 0.55 m were removed to filter out cross errors below or above the ground surface. The removed points were replaced using linear interpolation to estimate the terrain height from the z-coordinates of the neighbouring points. In addition, the terrain heights were smoothed using a moving 3 x 3 -pixel average filter.

The TLS point cloud was then normalized using the DTM. For each point in the point cloud, the nearest terrain point in the xy-plane was searched, and the corresponding terrain height was subtracted from the z-coordinate of the point. A sample of points was taken between 0 m and 1.0 m above the ground to be used in developing the method for downed dead wood detection and characterization. The lower limit of the height range was set to 0 cm, 5 cm, 10 cm and 15 cm, respectively, to investigate the parameter sensitivity. Based on sensitivity analysis, suitable value for lower limit was finally selected.

2.2.2 Automatic detection of downed dead wood trunks from the point cloud

Based on trunk geometry, the downed dead wood trunks were automatically detected from the normalized point cloud. It was presumed that a downed dead wood trunk could be distinguished from the undergrowth vegetation and other near-ground objects by means of its regular and cylindrical shape. Therefore, cylinder fitting, detailed surface modelling, and segmentation methods were utilized to automatically detect the downed dead wood trunks. The objective of the trunk detection was to determine the locations of the butt-end and top-end of each trunk, and eventually, be able to define the points from the point cloud representing each trunk. The automatic dead wood trunk detection method was a four-stage procedure comprising of: 1) point cloud filtering, 2) conversion of point cloud into a raster image, 3) segmentation of the raster image and segment classification, and 4) dead wood trunk positioning. A summary of main techniques used for point cloud processing is presented in Table 4. The method is described in detail in the next paragraphs.

Table 4. Main techniques used for point cloud processing in different stages of the automatic downed dead wood detection method.

Stage	Techniques
1. Point cloud filtering	- RANSAC cylinder fitting for removing the outlier points, performed in 0.5 m x 0.5 m grid.
2. Conversion of point clouds into raster images	- Point cloud projection onto xy-plane. - Raster image describing the point density: pixel size 2 cm x 2 cm. - Reclassification of raster values: one if point density ≥ 4 points/pixel. Otherwise zero. - Binary image processing: morphological opening and closing.

3. Raster image segmentation and segment classification	- Adjacent binary image pixels considered to form image regions (i.e., segments).
	- Calculation of segment properties describing the geometry through considering each segment as an ellipse:
	  - *Length of the major axis (length of the segment)*
	  - *Length of the minor axis (width of the segment)*
	  - *Eccentricity (ellipticity) of the segment*
	- Classification of the image segments to represent dead wood trunks based on the geometrical features: the minimum acceptable length and ellipticity.

4. Dead wood trunk positioning	- Deriving the xy-coordinates for the end-points and calculating the orientation of each segment. - Calculating the distance to the nearest neighboring dead wood segment - Calculating the angular difference between the segment orientation and the line intersecting both segment's mid-points. - Considering the segments representing the same trunk based on mutual position and orientation: the maximum acceptable distance and the angular difference in orientation. - Delineation of the points representing individual dead wood trunks based on segment width and end-points.

The objective of the point cloud filtering was to find the cylindrical structures of the point cloud which are assumed to represent the shapes of the downed dead wood trunks. First, the point cloud was divided into a 0.5 m x 0.5 m grid on the xy-plane, and a cylinder was fitted to the points in each grid cell. The cylinder fitting was based on the RANSAC-algorithm (Random Sample Consensus, see Bolles, Fischler 1981), which is commonly used when estimating parameters for mathematical models fitted in a data set that has outliers. From the dead wood detection point of view, the outliers are points representing the undergrowth vegetation and the branches. In the RANSAC-based cylinder fitting, a two-stage procedure is iteratively repeated. First, a random sample of points is selected, into which the cylinder is fitted. The cylinder fit is then evaluated by examining how well the fitted cylinder represents the rest of the points in the sample. Points within a defined maximum distance from the cylinder surface (i.e., inliers) form a consensus set and the iteration is repeated until the proportion of inliers in the consensus set corresponds to the desired level of confidence.

In the cylinder filtration process, the diameter of the fitted cylinder was limited to the range from 5 cm to 70 cm, which, based on 2014 field inventory, was the assumed range for the diameter of the dead wood trunks in the study area. Furthermore, the cylinder orientation was allowed to differ a maximum of 30° from the horizontal direction, to avoid detecting standing trees. Points within a maximum of 15 mm distance from the cylinder surface were considered as inliers, in other words, the points possibly representing the surfaces of downed dead wood trunks.

The second step of the dead wood detection method was to convert the filtered point cloud into a detailed raster image. The inlier points were projected onto xy-plane to construct a raster image with a 2 cm x 2 cm pixel size. The value of each pixel was calculated as the number of inlier points. Pixels with higher point density were assumed to more likely represent cylindrical dead wood trunk surfaces.

Therefore, the raster was converted into a binary image by re-classifying the pixel values. The pixel was given a value of one if the pixel included at least four inlier points. Otherwise, the pixel was given a value of zero (see Table 4). Consequently, the pixels with a value of one were indicating the areas on the sample plot that, based on cylindrical small-scale topography, were assumed to represent the locations of downed dead wood trunks. The binary image was further processed using morphological opening and closing operations (see, e.g., Beyerer et al. 2016) to strengthen the distinction of individual downed dead wood trunks from the other surrounding near-ground objects (Figure 3).

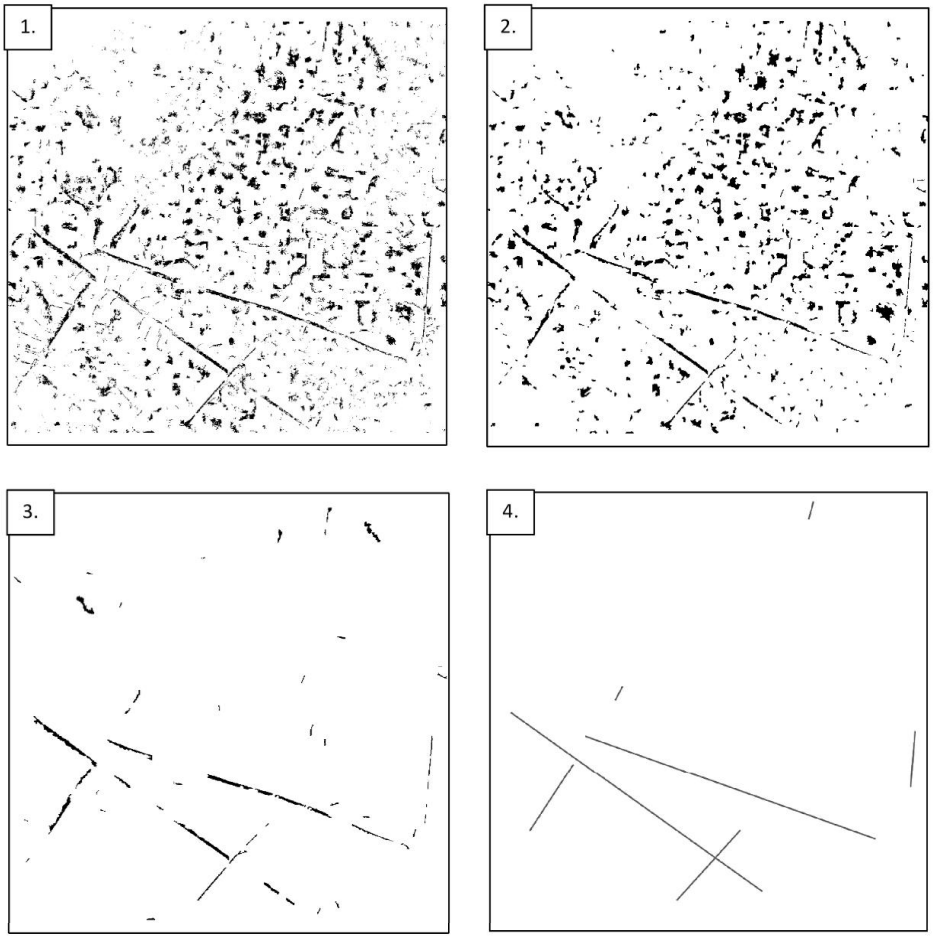

Figure 3. The stages of the automatic dead wood trunk detection procedure. First, the point cloud was filtered using RANSAC-based cylinder fitting, and the filtered point cloud was converted into a 2 cm x 2 cm binary raster image (1). The binary image was processed using filtering and morphological operations, and adjacent pixels were considered as segments (2). Geometrical features were calculated for the image segments, and strongly elliptical segments were then considered to represent the downed dead wood trunks (3). Based on the positions and the orientations of the image segments, the locations of the detected trunks were determined (4).

In the third step of the trunk detection procedure, the adjacent pixels were segmented and classified into segments representing dead wood trunks, and segments representing other near-ground objects. The classification was based on segment geometry, since segments representing downed dead wood trunks were found elliptical. In other words, the length of a dead wood trunk was typically several times larger than its diameter. Therefore, each image segment was considered as an ellipse, for which a set of features (i.e., length, width, and eccentricity of the segment) were computed (Table 4). The feature describing segment eccentricity, denoted as ε, was calculated as the ratio of the distance between the focal points (f) to the length of the major axis of the ellipse (a) (see Figure 4). At this point, the value for eccentricity is interpreted as follows: the more elliptical the segment is, the closer

the eccentricity is to one. To investigate an appropriate threshold for acceptable ellipticity, the minimum eccentricity was set to 0.97, 0.98, and 0.99, respectively. An image segment was classified to represent a dead wood trunk if the length of the segment exceeded 0.5 m and the eccentricity of the ellipse was higher or equal to the set minimum eccentricity (Figure 3).

The fourth stage of the automatic dead wood trunk detection method included the determination of trunk locations based on the line segments representing the major axes of the elliptical image segments. The trunks were represented either by a single continuous line segment or by a set of line segments, each representing a section of a trunk. The line segments representing the same trunk were searched and combined according to the following conditions. Line segment B was combined with line segment A if (1) the angle between the line segment A and a straight line intercepting the line segments A and B at their midpoints was 7° at the most and (2) if the distance between the line segments A and B was not more than 4 m. This procedure was repeated until the conditions were fulfilled. Eventually, the locations of the line segments with length of at least 1.0 m were considered to represent the locations of the downed dead wood trunks (Figure 3).

According to the locations of the automatically detected downed dead wood trunks, the points representing the trunks were delineated from the point cloud for further processing. The delineation was based on the width of the image segments, which was assumed to approximately represent the diameter of the dead wood trunk. Points within a distance equal to the length of the minor axis of the ellipsoidal image segment (see Figure 4), were considered as trunk points.

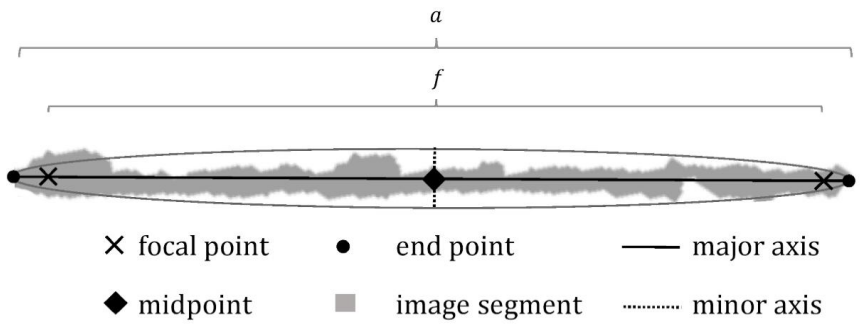

Figure 4. Each image segment was considered as an ellipse with two focal points. Major axis is the line segment that crosses the mid-point and both focal points of the ellipsoidal image segment, and is bounded by the end points of the segment. The ellipticity of the image segment is measured as the eccentricity of the ellipse, denoted as ε as a ratio of the distance between the focal points (f) to the length of the major axis (α).

2.2.3 Method for deriving the quantity and quality attributes for the detected trunks

After detecting the downed dead wood trunks from the point cloud, trunk attributes were automatically derived based on the points delineated separately for each detected trunk. For each trunk, the length and the trunk diameters were automatically measured to estimate the trunk volume. The length of the dead wood trunk was determined as the distance between the end points of the detected trunk. The diameters were estimated using a two-stage procedure including point cloud filtering and cylinder fitting. Point cloud filtering was conducted to distinguish the points representing a trunk from the points representing branches and other near-ground objects. The filtering was based on the direction of surface normal vector calculated for each point according to 30 neighbouring points. For the points representing the trunk surface, the surface normal vector was assumed to be roughly perpendicular to the trunk axis, i.e., parallel to the trunk axis normal vector. Therefore, the points were classified as trunk points if the angular deviation between the point surface normal and the trunk axis normal was not more than 5°.

The filtered point cloud representing each dead wood trunk was utilized for measuring diameters along the dead wood trunk at 10 cm intervals. A cylinder was fitted into a 15 cm wide slice of points (i.e., ±7.5 cm around each measuring point), and the trunk diameter was then derived as the diameter of the fitted cylinder (Figure 5). Despite the point cloud filtering, consecutive diameter observations tended to vary. The trunk surfaces were often covered with mosses, and hence, the filtration process did not always succeed in removing points representing the near-ground objects. Therefore, the trunk diameters were first filtered to remove outlier observations that originated from erroneous measurements (Figure 6). Diameter observations that deviated from the mean of all the diameters more than the standard deviation of the diameters were considered as outliers and thus removed. For smoothing the remaining diameter observations and interpolating the missing diameters along the trunk, a cubic spline curve was fitted (Figure 6). For the cubic spline curve, a smoothing parameter p determining the stage of smoothing was defined. If $p = 1$, the spline is converged to follow each observation in the data. The closer the value of p is to zero, the more the spline is flattened towards the linear least square estimate. Saarinen et al. (2017) found values 0.4–0.6 for the smoothing parameter p to be suitable for smoothing diameter-height observations for standing trees. Therefore, in this study, the value for p was set to 0.5 (Figure 6). After estimating the trunk diameters, the trunk volume was calculated using the Huber formula (Equation 1).

After estimating the length, mid-diameter and volume for each detected dead wood trunk, the attributes describing the quality and quantity of the downed dead wood at plot-level were calculated as a sum or mean of the trunk attributes. Total volume, as well as mean length, diameter, and volume were considered as plot-level attributes. In addition, a distribution of dead wood trunk mid-diameter was established to describe the quality and quantity of downed dead wood in the entire study area.

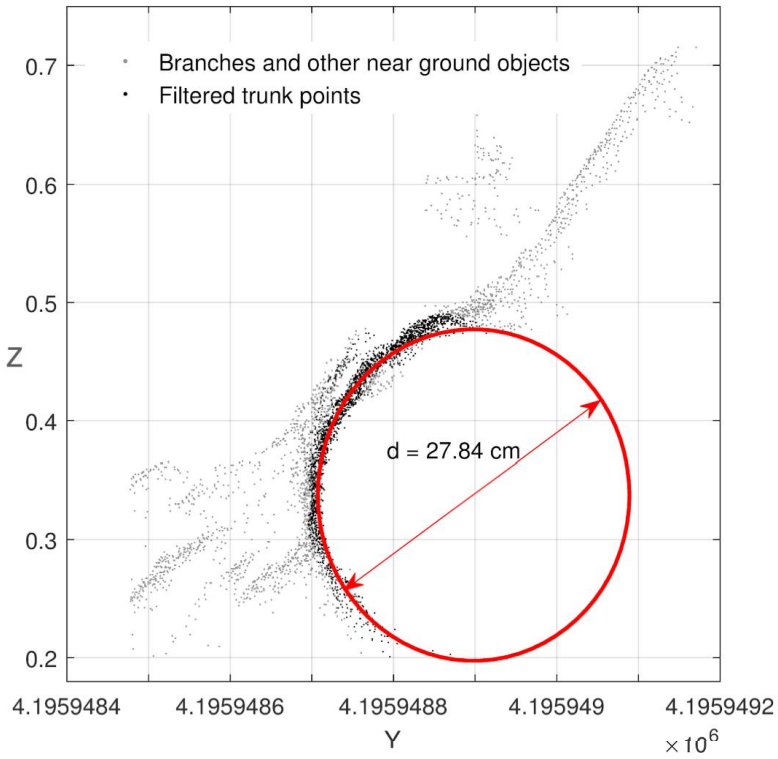

Figure 5. Two-dimensional representation of diameter estimation based on point cloud filtering and cylinder fitting. Diameters along the dead wood trunk are measured by fitting cylinders to filtered points that represent the trunk surface instead of branches and other near-ground objects. Diameter at each measuring spot is derived as the diameter of the fitted cylinder.

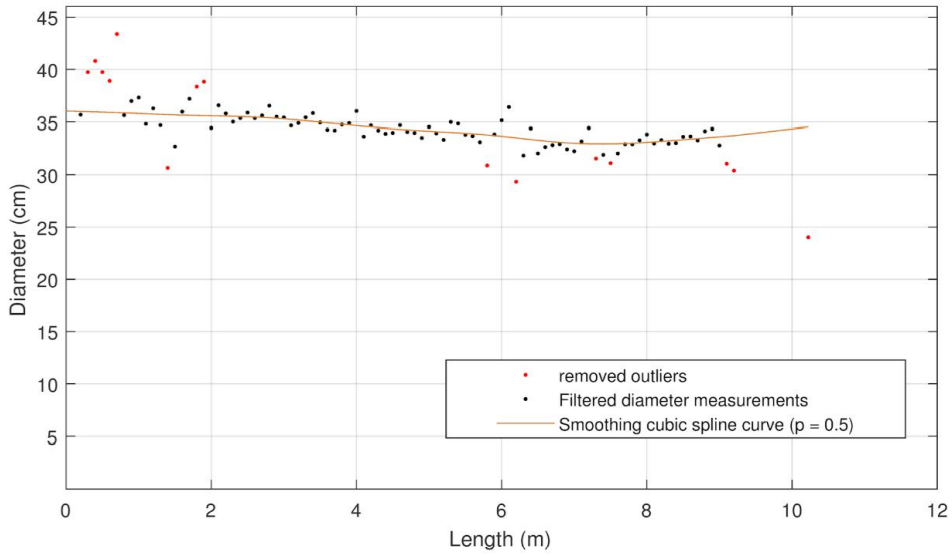

Figure 6. Outlier diameters are removed, and a cubic spline curve is fitted to smooth the filtered observations and to interpolate missing diameters.

2.3 Detection of downed dead wood trunks from the point cloud using visual interpretation

To assess the performance of the automatic dead wood detection method, downed dead wood trunks were detected from the original point clouds also by using visual interpretation. The visual interpretation of the point cloud was assumed to represent the highest level of accuracy that could be achieved from the point clouds. Here, the fundamental idea was that if the dead wood trunk is detected visually, it can also be detected automatically. On the contrary, if the trunk remains undetected using the visual interpretation, it is not reasonable to assume that the trunk could be detected using the automatic method either.

The visual interpretation of the point clouds was performed using Terrascan-software (Terrasolid Oy, Helsinki, Finland), where the point clouds were coloured according to the intensity of the back-scattered laser pulses. Line segments were then manually fitted into the point cloud to represent the locations of downed dead wood trunks on the sample plot. The xy-coordinates of the detected trunks were transferred as a text file into MATLAB, where the points representing downed dead wood trunks were delineated for further processing. Similarly, length, mid-diameter, and volume for individual trunks, as well as plot-level attributes were obtained by applying the same approach that was used for automatically identified dead wood trunks (see Section 2.2.3).

2.4 Assessing the performance of TLS-based method for mapping downed dead wood

Accuracy of both automatic and visual methods for mapping downed dead wood was first assessed at the plot-level. At the plot-level, the TLS-derived total volume of downed dead wood, as well as mean length, diameter, and volume of dead wood trunks were compared to validation measurements and assessed using bias (Equation 2) and root mean square error (RMSE, Equation 3):

$$bias = \frac{\sum_{i=1}^{n}(\hat{X}_i - X_i)}{n} \quad (2)$$

$$RMSE = \sqrt{\frac{\sum_{i=1}^{n}(\hat{X}_i - X_i)^2}{n}} \quad (3)$$

where n is the number of sample plots, $\hat{X}_i$ is the TLS-estimate for the plot-level dead wood attribute for plot i, and X_i is the corresponding attribute based on field reference. In addition, the relative values for bias and RMSE were computed by normalizing the values by the field-measured average.

Then, the accuracy of detecting individual dead wood trunks from point clouds were assessed at tree-level. This involved matching both automatically and visually detected trunks to the trunks measured in the field. As the data was relatively small, the trunk matching was based on visual interpretation which was aided with a map of standing trees. A dead wood trunk detected from the point cloud was considered to correspond a field-measured trunk if the location and orientation of the trunk matched with the tree map. If no correspondences were found, the trunk was considered as falsely detected. Completeness and correctness were used as measures to evaluate trunk detection accuracy at plot-level. Completeness measures the percentage of the field-measured reference trunks that was successively detected using the TLS-based method (Equation 4). Correctness indicates the percentage of the trunks detected using the TLS-based method that was correctly matched with reference trunks (Equation 5):

$$Completeness = \frac{n_{match}}{n_{ref}} \times 100\ \% \tag{4}$$

$$Correctness = \frac{n_{match}}{n_{TLS}} \times 100\ \% \tag{5}$$

where n_{match} is the number of correctly detected trunks, n_{ref} is the number of field-measured reference trunks and n_{TLS} is the number of trunks detected from the point cloud.

To evaluate the robustness of the method, the effects of various parameters on dead wood detection were investigated. The automatic detection method was applied using different combinations of values for parameters that were presumed to be most sensitive to dead wood detection (i.e., the lower limit to height above the ground in point cloud delineation and the minimum acceptable eccentricity for binary image segments). Other factors possibly affecting the detection accuracy were investigated by comparing the attributes of correctly detected trunks to the attributes of falsely detected trunks. The Student's t-test was utilized in examining whether there were statistically significant differences in the trunk dimensions between the detected and undetected trunks. Two-sample Kolmogorov–Smirnov test was used to investigate whether there were statistically significant differences in other quality attributes (i.e., species distribution, stage of decay, and bark coverage) between the detected and undetected trunks.

Accuracy assessment at trunk-level was based on comparison of TLS-estimates for individual trunk attributes (i.e., mid-diameter, length, and volume) to the reference measurements. The accuracy was evaluated by computing RMSE, as well as minimum, mean, and maximum difference between the TLS-estimates and the reference measurements. RMSE was derived using Equation 3 where n was now the number of trunks, $\hat{X}_i$ was the TLS-estimate for the individual trunk attribute for trunk i, and X_i was the corresponding attribute based on field reference. Difference was calculated by subtracting the reference value from the corresponding TLS-estimate. Arithmetic mean of the difference was hereby denoted as bias (see Equation 2). To achieve comparable results, the accuracy assessment at trunk-level was delineated to concern only the trunks that were correctly detected using both detection methods (i.e., automatic processing and visual interpretation). The accuracy assessment was conducted separately for both detection methods, not only to reveal the differences in the performance of the automatic and manual methods, but also to investigate the potential of TLS point clouds in mapping downed dead wood trunks.

3. RESULTS

3.1 Functionality of the developed method for mapping downed dead wood

Parameters used in various stages of the automatic detection of downed dead wood trunks affected the trunk detection. Two of the parameters (i.e., the lower limit to height above the ground in point cloud delineation and the minimum acceptable eccentricity for binary image segments) were found to have the most significant effect on the automatic dead wood detection. The effect of these parameters in trunk detection are illustrated in Figure 7. As the lower limit to the height above the ground in point cloud delineation and the minimum acceptable eccentricity of the image segments were increased, the correctness of the trunk detection was improved. Correspondingly, as the lower limit to the height above the ground in point cloud delineation was decreased and the minimum acceptable eccentricity of image segments was decreased, both the number of detected and falsely detected trunks were increased (Figure 7). Based on sensitivity analysis, values for the lower limit to the height above the ground and the threshold for minimum eccentricity were finally set to 15 cm and 0.98, respectively.

Mid-diameter distributions indicating the overall variation in downed dead wood is presented in Figure 8. The distributions derived using both automatic and visual detection of dead wood trunks reveal the performance of the TLS-based methods in characterizing downed dead wood. With both methods, the quantity of dead wood, especially in the smallest mid-diameter class (from 5 cm to 10 cm) was underestimated. Automatic dead wood detection resulted in systematic underestimation in mid-diameter classes from 5 cm to 40 cm. Visual interpretation of the point cloud improved the accuracy of the estimates in mid-diameter classes from 10 cm to 25 cm but led to overestimates in larger diameters.

3.2Accuracy of downed dead wood attributes at the plot level

By using the developed method, accuracy of estimates for downed dead wood volume varied at the plot level. The volume was underestimated on 18 sample plots while overestimation occurred on two sample plots. Absolute difference between the estimated and measured volume was 1.1 m^3/ha at the minimum and 30.8 m^3/ha at the maximum. On average, the volume was underestimated by 11.7 m^3/ha (46.2%) with an RMSE of 15.0 m^3/ha (59.3%) (Table 5). The accuracy of the estimates for total dead wood volume was improved by detecting the dead wood trunks visually from the point clouds. The minimum and maximum absolute difference between the estimated and measured downed dead wood volume were 0.3 m^3/ha and 15.4 m^3/ha, respectively. Using visual interpretation, the total volume was estimated with an RMSE of 6.4 m^3/ha (25.3%) while the bias was reduced to 0.4 m^3/ha (1.6%) (Table 5).

Differences in dead wood trunk detection between the automatic method and visual interpretation had only a slight effect on the accuracy of estimates for attributes describing the quality of downed dead wood at the plot level. The RMSE for estimates for mean mid-diameter, mean length, and mean trunk volume were 7.1 cm, 4.4 m, and 143.0 dm^3, respectively, when the estimates were based on automatic detection of dead wood trunks. Visual interpretation of the point cloud improved the accuracy of the estimate for mean length, as the respective RMSEs were 7.0 cm, 2.1 m, and 136.9 dm^3. Using both methods, the mean mid-diameter and mean trunk volume were overestimated, while the mean length was underestimated (Table 5).

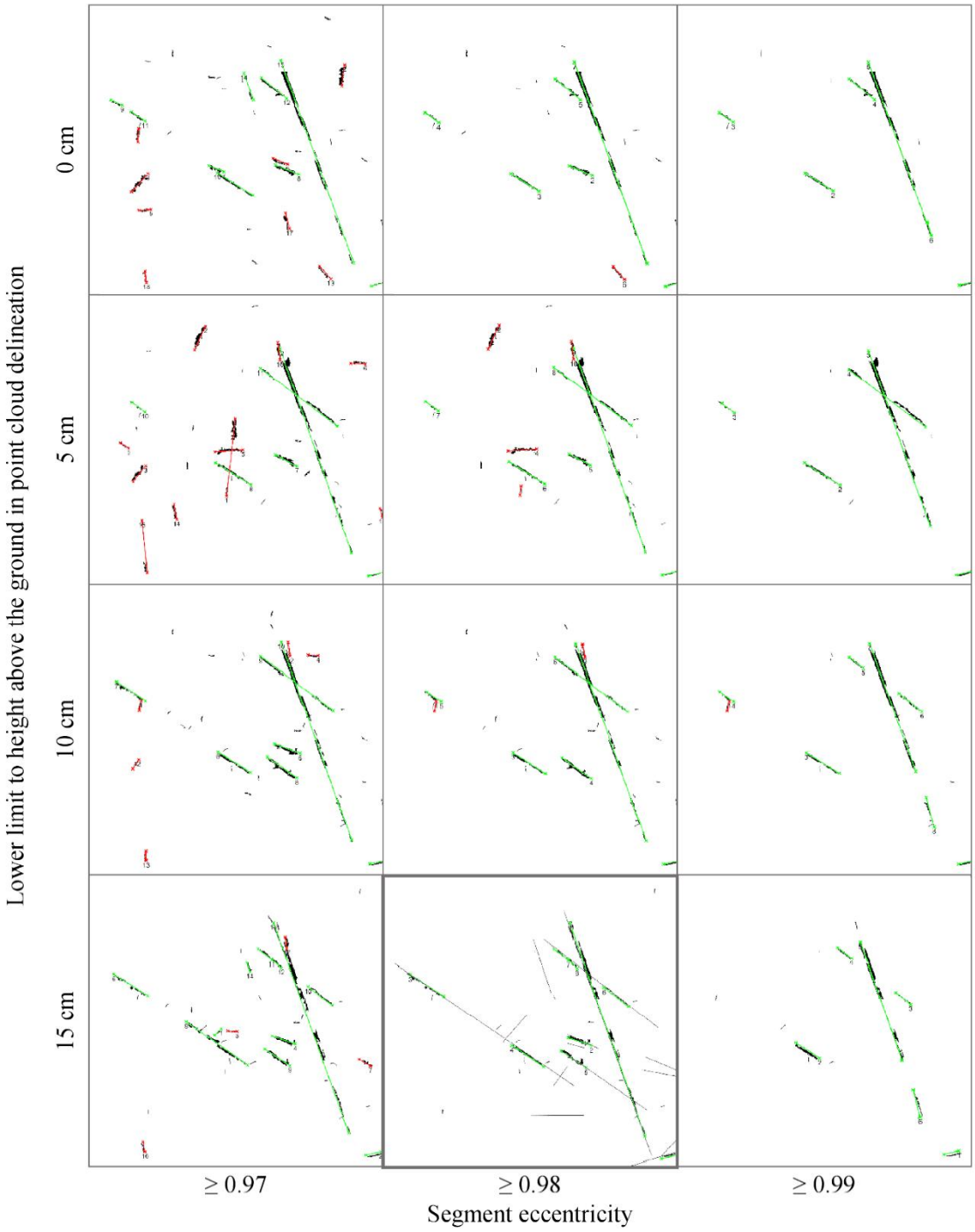

Figure 7. Downed dead wood trunks automatically detected from the TLS point cloud of a sample plot (32 m x 32 m) using different combinations of parameter values with the most significant effect on trunk detection. For each scenario, black segments are the binary image segments resulting from point cloud delineation, filtering, and surface model segmentation. Based on the segment eccentricity, they are considered to represent dead wood trunks. Green line segments indicate trunks detected from the point cloud and correctly matched with the reference trunks. Red line segments indicate falsely detected trunks. The figure with highlighted borders represents the result of trunk detection based on the parameter combination used in this study. In the highlighted figure, locations of field-measured reference trunks are marked with light grey line segments. From the 14 reference trunks on the presented sample plot, 6 trunks (43 %) were detected automatically and 10 trunks (71 %) based on visual representation of the point cloud. Lower limit to height above the ground used was 15 cm, and the minimum segment eccentricity 0.98.

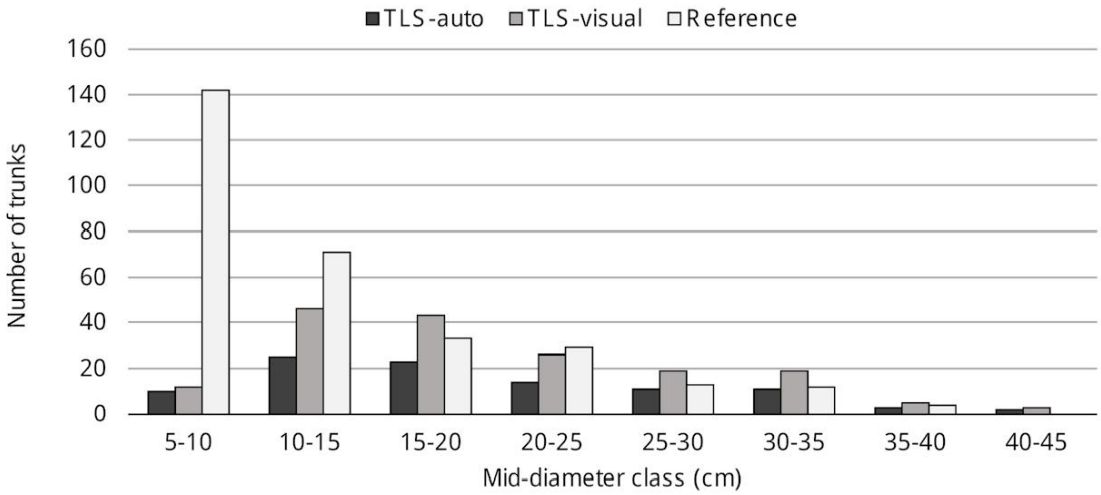

Figure 8. Measured and estimated mid-diameter distribution of downed dead wood trunks in the study area based on automatic (TLS-auto) and visual trunk detection (TLS-visual).

Table 5. Absolute and relative bias and root mean square error (RMSE) of attributes describing the quantity and quality of downed dead wood at plot-level using automatic method (TLS-auto) and visual interpretation (TLS-visual). Negative bias denotes underestimation.

	Bias		RMSE	
TLS-auto				
Total volume of downed dead wood (m^3/ha)	-11.7	-46.2%	15.0	59.3%
Mean mid-diameter of dead wood trunk (cm)	4.6	34.6%	7.1	53.4%
Mean length of dead wood trunk (m)	-2.2	30.6%	4.4	61.1%
Mean volume of dead wood trunk (dm^3)	34.7	20.4%	143.0	83.9%
TLS-visual				
Total volume of downed dead wood (m^3/ha)	0.4	1.6%	6.4	25.3%
Mean mid-diameter of dead wood trunk (cm)	6.3	47.4%	7.0	52.6%
Mean length of dead wood trunk (m)	-1.3	18.1%	2.1	29.2%
Mean volume of dead wood trunk (dm^3)	104.7	61.4%	136.9	80.3%

3.3 Accuracy of the downed dead wood detection

The overall completeness of the dead wood detection was 33% for the automatic procedure, i.e., one third of the field-measured downed dead wood trunks were correctly detected. However, the detected trunks represented 68% of the total dead wood volume. Visual interpretation of the point cloud improved the detection accuracy to 72% and the detected trunks represented 83% of the total dead wood volume. Correctness of the trunk detection was similar for both methods varying from 75% to 76 % (Table 6). It should be noted that the detection accuracy varied between the sample plots. Using visual interpretation, on two sample plots all the dead wood trunks were detected. On these plots, the number of dead wood trunks was 5 and 9. The mid-diameters of the trunks were ranging from 6.2 cm to 18.3 cm and from 6.8 cm to 24.1 cm while the lengths of the trunks were ranging from 3.0 m to 17.5 m and from 3.0 m to 20.0 m, respectively. These sample plots were characterized by sparse undergrowth vegetation resulting a good visibility. The highest completeness obtained using automatic detection was 60 % (3/5 trunks detected) and it was obtained on the first of the abovementioned sample plots. However, when considering the detection accuracy as a proportion of detected dead wood volume from the total dead wood volume, the highest performance of the automatic detection method was obtained in an old-growth forest. This sample plot was characterized

by a diverse variety of dead wood trunks with mid-diameters ranging from 5.0 cm to 33.4 cm and lengths ranging from 2.2 m to 28.0 m, where the largest dead wood trunks represented most of the total dead wood volume. From this sample plot, 6 dead wood trunks were detected out of 14, representing 92% of the total volume and 82% of the total length of the downed dead wood trunks.

Table 6. Completeness and correctness of downed dead wood detection based on automatic method (TLS-auto) and visual interpretation of TLS point cloud (TLS-visual). Detected volume indicates the percentage of the detected volume of dead wood from the total dead wood volume. Percentages in parenthesis illustrate the variation between the sample plots.

	Completeness	Correctness	Detected volume
TLS-auto	33% (0–60%)	76% (50–100%)	68% (0–92%)
TLS-visual	72% (33–100%)	75% (45–100%)	83% (11–100%)

Dimensions of downed dead wood trunks affected the detection accuracy. The larger the dimensions were, the more reliable was the trunk detection. The effect of trunk dimensions (i.e., mid-diameter and length) on trunk detection are illustrated in Figures 9 and 10. Based on the visual interpretation, 65% of the trunks with mid-diameter ranging from 5 to 10 cm were detected, whereas for the largest trunks (35 cm – 40 cm) 100% of the trunks were detected. Using the automatic method, 19% and 75% of the trunks were detected, respectively (Figure 9).

Besides mid-diameter, the length of the trunk was also affecting the trunk detection. Based on the visual interpretation, 57% of the trunks with length less than 2 m were detected, whereas the trunks with length over 15 m were all detected. Using the automatic trunk detection procedure, 10% of the trunks with length under 2 m were detected, while the respective figure for the completeness for the longest trunks was 83% (Figure 10).

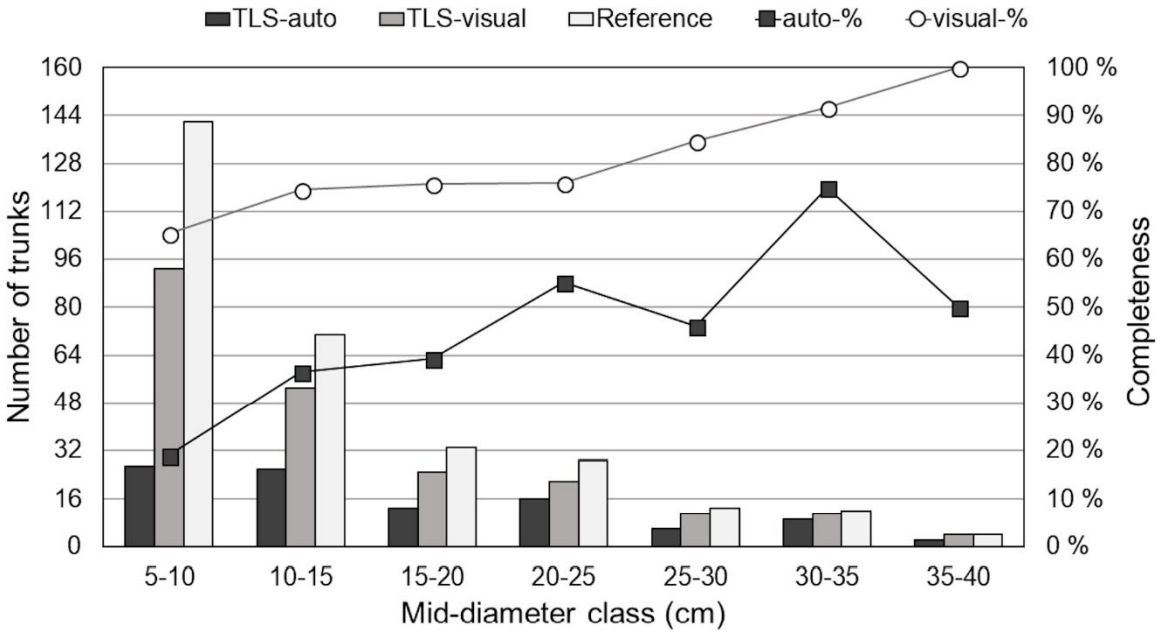

Figure 9. Downed dead wood detection accuracy with respect to the mid-diameter of a dead wood trunk. Bars represent the number of detected trunks in each mid-diameter class and lines represent the respective completeness of the trunk detection.

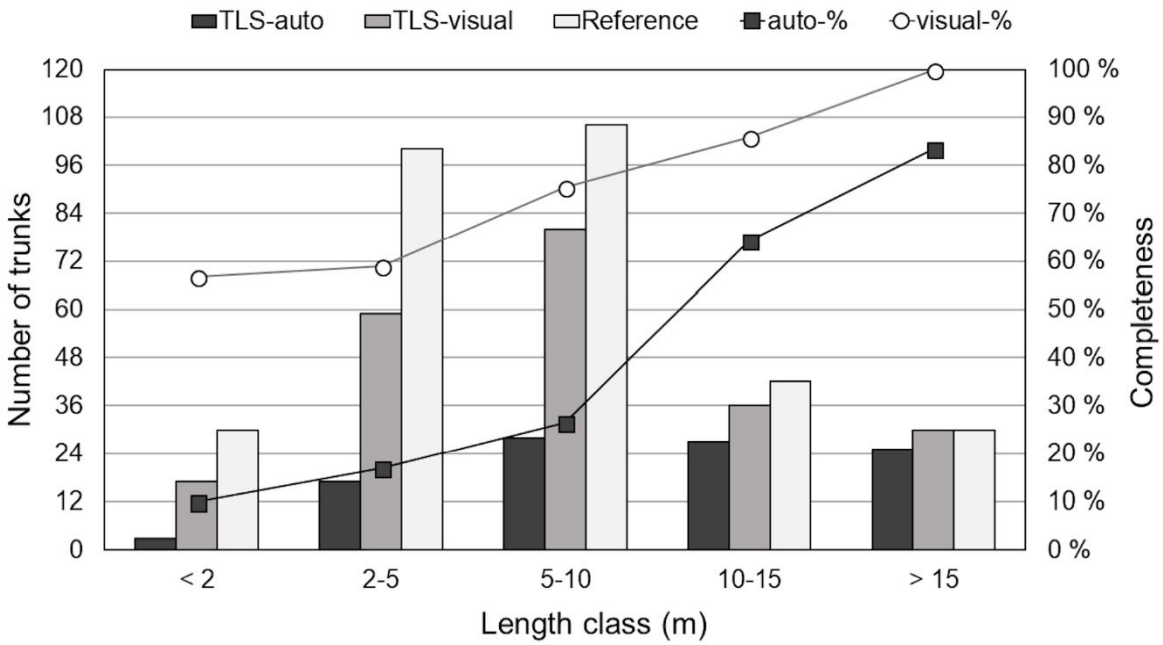

Figure 10. Downed dead wood detection accuracy with respect to the length of a dead wood trunk. Bars represent the number of detected trunks in each length class and lines represent the respective completeness of the trunk detection.

Altogether, 205 dead wood trunks, which stands for 67% of all the reference trunks, were not detected by the automatic method. Of the 205 undetected trunks, 85 trunks (42%) remained undetected even when using the visual interpretation. Trunk dimensions were found to be the most significant factors affecting the failure in detecting the trunks, as is shown in Figures 9 and 10. Mid-diameter, length, and volume of the detected trunks were higher than the corresponding attributes of undetected trunks (Table 7). In addition, for the automatically detected trunks, the median mid-diameter was 2.9 cm larger and the median length 3.6 m larger than the respective figures for the visually detected trunks. Based on the Student's *t*-tests, the differences of these attributes were statistically significant ($p < 0.05$) between the two methods. According to Kolmogorov–Smirnov tests, other dead wood quality attributes (e.g., tree species, stage of decay, and bark coverage) did not have statistically significant effect on the detection accuracy ($p > 0.05$).

Table 7. Variation of attributes of downed dead wood trunks detected and undetected from the TLS point clouds using automatic detection method (TLS-auto) and visual interpretation of point clouds (TLS-visual).

	Detected			Undetected		
	mid-diameter (cm)	length (m)	volume (dm^3)	mid-diameter (cm)	length (m)	volume (dm^3)
TLS-auto		n = 99			n = 205	
min	5.3	1.2	3.4	5.0	0.9	3.5
median	14.4	10.4	146.9	9.0	4.5	32.8
max	39.5*	28.0	2550.0	39.5*	19.3	1056.6
standard dev.	8.6	6.5	466.9	6.7	3.5	143.9
TLS-visual		n = 219			n = 85	
min	5.0	0.9	3.4	5.0	1.0	4.7
median	11.5	6.8	70.8	8.5	3.7	24.2
max	39.5	28.0	2550.0	33.4	13.8	354.7
standard dev.	8.1	5.8	361.6	5.9	2.9	71.7

* The detected and undetected trunks with mid-diameters of 39.5 cm had lengths of 9.0 m and 1.0 m, respectively.

3.4 Accuracy of tree-level attributes

Of all the 304 field-measured dead wood trunks, 94 were detected using both automatic detection procedure and visual interpretation of point clouds. On average, these trunks had a larger mid-diameter and length than all the field-measured dead wood trunks. The median mid-diameter was 14.5 cm and the median length 10.6 m, as the respective figures for all the trunks were 10.5 cm and 5.9 m (see Table 3). The accuracy of estimating individual trunk attributes for the above mentioned 94 trunks is presented in Table 8. RMSE of estimating the mid-diameter for individual dead wood trunk was 5.7 cm using the automatic detection procedure, and 6.0 cm using the visual interpretation of point clouds. The mid-diameter was overestimated by 3.2 cm for the automatic detection and by 4.1 cm for the visual interpretation. Based on the visual interpretation, RMSE in estimating length and volume were 3.9 m and 201.7 dm^3, respectively. The corresponding figures for automatic detection were 7.2 m and 305.7 dm^3. Trunk volume was underestimated using the automatic method, while the visual detection overestimated the volumes. The length of the trunks was underestimated regardless of the detection method.

Table 8. Accuracy of individual downed dead wood attributes using automatic detection method (TLS-auto) and visual interpretation (TLS-visual). Negative difference denotes underestimation.

	RMSE	Difference		
		min	mean (bias)	max
TLS-auto				
mid-diameter (cm)	5.7	-10.35	3.2	17.9
length (m)	7.2	-20.87	-5.5	3.8
volume (dm^3)	305.7	-1321.07	-100.7	1019.9
TLS-visual				
mid-diameter (cm)	6.0	-6.22	4.1	29.8
length (m)	3.9	-11.81	-2.6	6.7
volume (dm^3)	201.7	-735.82	66.3	707.5

4. DISCUSSION

The objective of this study was to develop an automatic method for detecting and characterizing downed dead wood by means of TLS point clouds. Using the developed method, 68% of the total volume of dead wood with mid-diameter larger than 5 cm were automatically detected. Given that larger dead wood trunks are more important for biodiversity than trunks with smaller dimensions (Söderström 1988; Andersson and Hytteborn 1991; Bader et al. 1995), the quantity of ecologically the most valuable dead wood was captured rather well, as 86% of the total volume of downed dead wood with mid-diameter larger than 30 cm were automatically detected. However, if the aim is to conduct a thorough dead wood inventory and to derive as accurate estimate as possible for the total quantity of downed dead wood at plot-level, it seems that the automatic dead wood detection can be aided with visual interpretation of point clouds. Besides detecting the trunks, spatial location, as well as the attributes describing the dimensions and quality of individual dead wood trunks were automatically derived using the developed method. Based on individual trunk attributes, a map of downed dead wood distributed in the sample plot was constructed along with the plot-level attributes on the quantity and quality of downed dead wood. Finally, a distribution of mid-diameters of downed dead wood trunks in the study area was derived.

The results of this study are in line with the previous findings presented by Polewski et al. (2017) who recently introduced a voting-based method to detect fallen trees from TLS point clouds. Polewski et al. (2017) examined the performance of their method on three sample plots and reported up to about 70–80% of length completeness which measures how large part of the total length of all fallen trees

were detected. However, the results are not directly comparable to this study, since the study site and reference data differ from each other. In Polewski et al. (2017), the reference data was solely based on visual interpretation of point clouds, and the sample plots were characterized by rather low density of living trees (81–339 trees/ha) with fallen trees notably larger in stem diameter (median 25–47 cm) than in the present study (342–2041 trees/ha, and 6.3–18.8 cm, respectively). Nevertheless, a length completeness of up to 82% was achieved in this study with the proposed method for a sample plot in an open mature forest with median dead wood trunk diameter of 16.0 cm. Further, if the reference data were defined according to the visual interpretation of point clouds, the respective length completeness would be even higher. Considering these facts, this study demonstrates a slightly improved performance in detecting downed dead wood automatically from the TLS point clouds.

The methodology behind the TLS-based mapping of downed dead wood is, in principle, similar to the mapping of standing trees with TLS point clouds. Individual trees are first detected, and tree attributes are then estimated from the tree-wise point clouds in order to achieve the plot-level attributes. However, there a few key differences between the methodologies. In general, standing tree stems are detected from TLS point clouds based on a horizontal point cloud slice where the cross-sections of trees are visible and detected by fitting a circle or a cylinder to the points (Aschoff and Spiecker 2004; Maas et al. 2008). Another common approach for standing tree detection is point cloud classification based on properties of the point neighbourhood (Liang et al. 2012; Raumonen et al. 2015). Depending on the forest structure, about 60% to 100% of the standing trees can be automatically detected (see, e.g., Maas et al. 2008; Liang et al. 2016), and the percentage of the detected volume can be assumed to be slightly higher. With respect to these figures, the volume of downed dead wood was detected almost as accurately with the developed method, although the conditions for detecting downed dead wood are even more challenging. Unlike the living trees that stand rather freely on vertical positions, downed dead wood trunks are lying on the forest floor among undergrowth vegetation and stones with less surface directly visible to the scanner.

One of the most significant factors affecting the dead wood trunk detection using the TLS-based methods was the size of the trunks. Detected trunks had a larger mid-diameter and length than the undetected trunks (Table 7), and similar finding was also reported by Polewski et al. (2017). Downed dead wood trunks form small-scale elevations that are distinguished from the undergrowth vegetation, stones, and other near-ground objects because of their cylindrical and regular shape. When lying on the ground, the trunk diameter determines the contrast of near-ground elevation adjunct to the trunk surroundings. Increase in diameter increases the elevation contrast promoting the distinction of a trunk. From a methodological point of view, the trunk surface must reach above the height threshold applied in vertical point cloud delineation (see Section 2.2.1). Thus, a dead wood trunk will not be detected if it remains below the threshold height which was eventually set to 15 cm in our study. This results with the possibility that the point cloud structures representing the small-diameter dead wood trunks may be excluded from the further analyses, which explains the poor performance of the method to detect small-diameter dead wood. Lowering the height threshold may improve the detection of small-diameter dead wood but with the cost of method robustness (i.e., correctness) (see Figure 7). Besides diameter, the length of a dead wood trunk also affects the detection accuracy, since long trunks with more surface visible to the scanner appear more continuous surfaces being more distinguishable than short trunks. Nevertheless, among the undetected trunks, there were also trunks that were considered large based on the dimensions. For example, a dead wood trunk with the largest volume among the undetected trunks (354.7 dm^3) had a mid-diameter of 23.5 cm and a length of 10 m. Most likely, the trunk remained undetected because it was occluded by dense undergrowth vegetation between the trunk and the scanner. Consequently, besides the dimensions of dead wood trunks, the quality of the point cloud is an essential factor affecting the dead wood detection, and thus, the mapping accuracy.

Forest structure has been reported to affect the accuracy of detecting standing trees from TLS point clouds since the trees shadowed by other trees and undergrowth vegetation remain undetected (Kankare et al. 2015; Abegg et al. 2017). The same phenomenon was also found to affect the dead wood detection. Even if the sample plots were scanned using five scanning positions, it was inevitable that some of the field-measured dead wood trunks were shadowed by the standing trees and undergrowth vegetation. At this point, it should be pointed out that the geometry of the scanning positions was not always optimal from the viewpoint of dead wood mapping since the scanning geometry was originally designed for mapping standing trees. The spatial distribution of downed dead wood is often irregular (Siitonen 2001), in which case it might not be feasible to collect the TLS data by placing the scanners evenly on the sample plot. Therefore, the detection accuracy is expected to be improved if the point cloud is collected to exhaustively cover all the dead wood on the sample plot. However, when forests are measured using TLS, both standing trees and downed dead trees should be detected and characterized. In most of the applications, excluding research, it is probably more important to be able to characterize standing trees as well as possible. Recognizing these requisites, it still seems that it is possible and worthwhile to use the terrestrial point cloud data also for dead wood mapping in addition to the inventory of standing trees.

Along with the trunk detection, various error sources in trunk attribute estimation affected the accuracy of TLS-based dead wood mapping. Accuracy of trunk length estimation was dependent on trunk detection as the length was determined from the part of the trunk that was detected from the point cloud. On average, the trunk length was underestimated since the trunk could not be detected exactly from the butt-end to top-end. With improved dead wood trunk detection, visual interpretation resulted in more accurate estimates for trunk length (see Table 8). Diameters, on the other hand, were estimated by fitting cylinders along the dead wood trunk. Similar method is commonly applied when measuring standing tree variables, as circle or cylinder fitting is used to derive stem diameters (e.g., Maas et al. 2008; Liang et al. 2014a; Calders et al. 2015; Saarinen et al. 2017). In case of standing trees, the RMSE of DBH estimation typically varies from sub-centimetre-level to some centimetres in boreal forests (see, e.g., Liang et al. 2016; Kankare et al. 2017). Given that the detection and characterization of downed dead wood includes more uncertainties as the trunks are located on the forest floor covered with epiphytes, the accuracy for mid-diameter estimation (~6.0 cm) can be considered acceptable. On average, the mid-diameters were overestimated, which is partly explained by the trunk detection. Even if the diameter measurement itself was unbiased, the measurement could occur at different section of the trunk with respect to the field-measured mid-diameter. The reference measurement for mid-diameter was based on a diameter measured exactly at the middle of the trunk. When applying the TLS-based method, the mid-diameter was derived from the middle of the detected trunk section. Often, some part of the trunk was not detected, which resulted in determining the mid-diameter at different point than the reference. On the other hand, estimates for mid-diameter and volume were based on the filtered and smoothed diameter-length observations which was assumed to decrease the effect of single erroneous observations. The procedure for filtering erroneous diameter measurements was incapable for detecting single outliers. Still, the aim of this study was not to construct perfect stem curves for dead tree trunks. More importantly, the objective was to automatically produce a sufficient amount of reliable diameter measurements along the trunk which could be smoothed and interpolated to estimate trunk volume and mid-diameter. It should also be noted that the reference data collected in the field did not include as dense diameter measurements as it is possible to automatically derive from the TLS point cloud. Anyway, the accuracy of estimates for mid-diameter and length are expected to be improved along with more accurate dead wood detection.

Besides the dead wood detection and trunk attribute estimation, the accuracy of the TLS-based dead wood mapping is affected by a set of assumptions and parameters used in various stages of the automatic mapping procedure. The trunk detection method is based on an assumption that the downed dead wood trunks are distinguished from the point cloud based on their regular and cylindrical shape

elevating from the ground. A dead wood trunk is not detected if its three-dimensional structure in the point cloud differs from this assumption. Correspondingly, small-scale topography of the forest stand (e.g., stones and hummocks covered with mosses) can be falsely identified as dead wood trunks if the appearance in the point cloud matches the definition. Parameters most significantly affecting the mapping accuracy were the ones controlling the classification of small-scale cylindrical topography into dead wood trunks (see Figure 7). However, parameter optimization was not the main objective of this study since the selection of parameter values, and thus the functionality of the mapping method can also be affected by forest stand conditions. It should also be kept in mind that the performance of the proposed method cannot be guaranteed with the given parameter values if the point cloud properties significantly differ from the ones used in this study.

In general, the sample plots used in this study were unrepresentative of typical forests in southern Finland. On average, the quantities of both living trees and downed dead wood on the selected sample plots were notably higher than in a typical forest stand in the area. Based on the latest results of Finnish National Forest Inventory, the mean volume of downed dead wood in southern Finland is 2.5 m^3/ha, whereas the respective figure for the sample plots used in this study was 25.3 m^3/ha (see Table 2). Therefore, the RMSEs achieved in this study are not directly comparable to other studies. Considering the applicability of the developed method, downed dead wood mapping could be expected to achieve the represented level of accuracy on forest stands that are structurally similar to the sample plots of this study. Given that the correctness of the dead wood detection was relatively high, it is assumed that an adequate level of accuracy is achieved when the automatic method is applied to sample plots with less downed dead wood as well.

When comparing the TLS-based dead wood mapping with mapping methods based on other remote sensing materials, the main advantage of the TLS-based method is its ability to provide tree-level information on downed dead wood. Methods utilizing ALS data and individual tree detection are capable of detecting only the largest fallen trees (see, e.g., Lindberg et al. 2013; Nyström et al. 2014). More detailed mapping of downed dead wood trunks requires bi-temporal ALS-data, as well as information on the forest stand history (Tanhuanpää et al. 2015). The comparison of dead wood mapping methods utilizing remote sensing materials involves considering the scale of the mapping. With optical remote sensing and ALS, it is possible to cover large areas, while TLS is suitable for data collection at tree or plot-level, and thus, for producing ground-truth data for large area mapping. Collecting TLS-data covering whole forest stands is laborious as, for example, one hectare requires dozens of individual scans. However, a laser scanner can be mounted on a moving platform (MLS, mobile laser scanning) to improve the cost-efficiency of terrestrial point cloud acquisition (Kukko et al. 2012; Liang et al. 2014b).

Additional benefits can be achieved when using the TLS-based dead wood mapping method instead of traditional field inventory. Deriving locations and orientations of downed dead wood trunks using conventional methods is laborious but can be automated using the TLS-based method. TLS point cloud can also be utilized, e.g., in describing the structure of a forest stand to aid the mapping of favourable environments for saproxylic species. However, the quality attributes of a dead wood trunk that are independent from trunk dimensions are challenging or even impossible to determine automatically from TLS point clouds. For example, measuring the stage of decay of a dead wood trunk cannot be reliably determined solely based on the trunk appearance, since information on the inner properties of the trunk is needed. Nonetheless, TLS provides information on back-scattered laser intensity, which aids the visual interpretation of point clouds and, for example, the assessment of bark coverage or other visible dead wood quality properties. It is also possible to obtain spectral information by colouring the point cloud based on a digital photograph or by using multi-spectral TLS (see, e.g., Junttila et al. 2018). Applying laser intensity and spectral information may improve the dead wood detection in occasions where the downed trees are more distinct and maybe not covered with epiphytes.

Detailed and up-to-date information on the quality and quantity of dead wood is needed to assess the forest biodiversity and carbon storage. The quantity of dead wood with diverse quality is interrelated with forest biodiversity since dead wood maintains the biodiversity by offering habitat for many threatened species in a boreal forest ecosystem (Harmon et al. 1086; Franklin et al. 1987; Esseen et al. 1997; Siitonen 2001). So far, traditional field inventory has been the only way to obtain precise information on the quantity and quality of dead wood. Still, during the last decade, the remote sensing-based methods have become more common in other forest inventory and mapping applications (Holopainen et al. 2014). TLS has proven to be an effective method collecting three-dimensional data for plot-level measurements of standing trees (e.g., Maas et al. 2008; Calders et al. 2015; Liang et al. 2016) and according to the results of this study along with the findings by Polewski et al. (2017), also for detecting and characterizing downed dead wood. The procedure for mapping downed dead wood using TLS point cloud is possible to be automated, which improves the practical applicability of the mapping method.

5. CONCLUSIONS

This study highlights the feasibility of TLS in mapping forest biodiversity indicators by introducing an automated method for quantifying downed dead wood and providing information on the dead wood quality attributes. The results of this study strengthen the feasibility of TLS-based approaches in mapping biodiversity indicators by demonstrating an improved performance in quantifying ecologically most valuable downed dead wood in diverse southern boreal forest conditions.

If TLS point clouds are acquired for mapping and measuring standing trees, downed dead wood can be detected and characterized simultaneously. According to the results, majority (68%) of the dead wood volume was detected using the automatic method. The accuracy of downed dead wood mapping was affected most by the detection of individual dead wood trunks. The reliability of dead wood mapping was found to increase alongside the dimensions of dead wood trunks. Mid-diameter of dead wood trunks was estimated with an adequate accuracy (RMSE ~6 cm) given that the trunks were lying on the forest floor among undergrowth vegetation, stones and other near-ground objects. The overall mapping accuracy is expected to be improved by reconsidering the scanning setup and taking the spatial distribution of downed dead wood into account.

The automated method for downed dead wood mapping performs the best in mature forests with easily-detectable large-sized dead wood trunks and with sparse undergrowth vegetation. If the objective is to achieve information regarding the quantity of ecologically most valuable dead wood and the quality attributes that are based on trunk dimensions, TLS-based mapping method is a noteworthy option for traditional field inventory. However, further investigation is needed to assess the feasibility of TLS to provide information on other dead wood quality attributes such as tree species and stage of decay.

ACKNOWLEDGEMENTS

The study was funded by the Academy of Finland through the Centre of Excellence in Laser Scanning Research (project number 272195) in co-operation with Beetles LIFE (LIFE17NAT/FI/000181). The authors would also like to thank Häme University of Applied Sciences for supporting the research activities at Evo study site.

DECLARATION OF INTEREST

The authors declare no conflict of interest.

REFERENCES

Abegg, M., Kükenbrink, D., Zell, J., Schaepman, M.E., Morsdorf, F., 2017. Terrestrial Laser Scanning for Forest Inventories – Tree Diameter Distribution and Scanner Location Impact on Occlusion. Forests 8(6), 184–213. http://dx.doi.org/10.3390/f8060184

Åkerblom, M., Raumonen, P., Mäkipää, R., Kaasalainen, M., 2017. Automatic tree species recognition with quantitative structure models. Remote Sensing of Environment, 191, 1-12. http://dx.doi.org/10.1016/j.rse.2016.12.002

Andersson, L.I., Hytteborn, H., 1991. Bryophytes and decaying wood–a comparison between managed and natural forest. Ecography, 14(2), 121-130. http://dx.doi.org/10.1111/j.1600-0587.1991.tb00642.x

Aschoff, T., Spiecker, H., 2004. Algorithms for the automatic detection of trees in laser scanner data. International Archives of Photogrammetry, Remote Sensing and Spatial Information Sciences 36(8), 72–75.

Bader, P., Jansson, S., Jonsson, B.G., 1995. Wood-inhabiting fungi and substratum decline in selectively logged boreal spruce forests. Biological conservation, 72(3), 355-362. http://dx.doi.org/10.1016/0006-3207(94)00029-P

Beyerer, J., Puente León, F., Frese, C., 2016. Morphological Image Processing. In: Beyerer, J., Puente León, F., Frese, C. (Eds.), Machine Vision. Springer, Berlin, Heidelberg, pp. 607–647. http://dx.doi.org/10.1007/978-3-662-47794-6_12

Bolles, R. C., Fischler, M. A., 1981. A ransac-based approach to model fitting and its application to finding cylinders in range data. Proceedings of the 7th International Joint Conference on Artificial Intelligence, 637–643.

Bütler, R., Schlaepfer, R., 2004. Spruce snag quantification by coupling colour infrared aerial photos and a GIS. Forest Ecology and Management, 195(3), 325-339. http://dx.doi.org/10.1016/j.foreco.2004.02.042

Cabo, C., Ordóñez, C., López-Sánchez, C.A., Armesto, J., 2018. Automatic dendrometry: Tree detection, tree height and diameter estimation using terrestrial laser scanning. International Journal of Applied Earth Observation and Geoinformation, 69, 164-174. http://dx.doi.org/10.1016/j.jag.2018.01.011

Calders, K., Newnham, G., Burt, A., Murphy, S., Raumonen, P., Herold, M., Culvenor, D., Avitabile, V., Disney, M., Armston, J., Kaasalainen, M., 2015. Nondestructive estimates of above-ground biomass using terrestrial laser scanning. Methods in Ecology and Evolution 6(2), 198–208. http://dx.doi.org/10.1111/2041-210X.12301

Danson, F.M., Gaulton, R., Armitage, R.P., Disney, M., Gunawan, O., Lewis, P., Pearson, G., Ramirez, A.F., 2014. Developing a dual-wavelength full-waveform terrestrial laser scanner to characterize forest canopy structure. Agricultural and Forest Meteorology, 198, 7-14. http://dx.doi.org/10.1016/j.agrformet.2014.07.007

Dassot, M., Constant, T., Fournier, M., 2011. The use of terrestrial LiDAR technology in forest science: application fields, benefits and challenges. Annals of forest science, 68(5), 959-974. http://dx.doi.org/10.1007/s13595-011-0102-2

Esseen, P.-A., Ehnström, B., Ericson, L., Sjöberg, K., 1997. Boreal forests. Ecological Bulletins 46, 16–47.

Fleck, S., Obertreiber, N., Schmidt, I., Brauns, M., Jungkunst, H.F., Leuschner, C., 2007. Terrestrial lidar measurements for analysing canopy structure in an old-growth forest. International Archives of Photogrammetry, Remote Sensing and Spatial Information Sciences, 36(Part 3), W52.

Franklin, J.F., Shugart, H.H., Harmon, M.E., 1987. Tree death as an ecological process. BioScience 37, 550–556. http://dx.doi.org/10.2307/1310665

Harmon, M.E., Sexton, J., 1996. Guidelines for Measurements of Woody Debris in Forest Ecosystems. Pub. No. 20. US LTER Network Office, Univ. of Washington, Seattle, WA. 73 pp.

Harmon, M.E., Franklin, J.F., Swanson, F.J., Sollins, P., Gregory, S.V., Lattin, J.D., Andersson, N.H., Cline, S.P., Aumen, N.G., Sedell, J.R., Lienkaemper, G.W., Cromack, K. Jr., Cummins, K.W., 1986. Ecology of coarse woody debris in temperate ecosystems. Advances in Ecological Research 15, 133–302. http://dx.doi.org/10.1016/S0065-2504(08)60121-X

Heinzel, J., Huber, M.O., 2016. Detecting tree stems from volumetric TLS data in forest environments with rich understory. Remote Sensing, 9(1), 9. http://dx.doi.org/10.3390/rs9010009

Henning, J.G., Radtke, P.J., 2006. Ground-based laser imaging for assessing three-dimensional forest canopy structure. Photogrammetric Engineering & Remote Sensing, 72(12), 1349-1358. http://dx.doi.org/10.14358/PERS.72.12.1349

Holopainen, M., Vastaranta, M., Hyyppä, J., 2014. Outlook for the next generation's precision forestry in Finland. Forests 2014(5), 1682–1694. https://doi.org/10.3390/f5071682

Ishak, N.I., Abu Bakar, M.A., Abdul Rahman, M.Z.A., Rasib, A.W., Kanniah, K.D., Meng Shin, A.L., Razak, K.A., 2015. Estimating single tree stem and branch biomass using terrestrial laser scanning. Jurnal Teknologi, 77(26), 59-67. http://dx.doi.org/10.11113/jt.v77.6860

Jonsell, M., Weslien, J., 2003. Felled or standing retained wood—it makes a difference for saproxylic beetles. Forest Ecology and Management, 175(1-3), 425-435. http://dx.doi.org/10.1016/S0378-1127(02)00143-3

Junttila, S., Sugano, J., Vastaranta, M., Linnakoski, R., Kaartinen, H., Kukko, A., Holopainen, M., Hyyppä, H. and Hyyppä, J., 2018. Can Leaf Water Content Be Estimated Using Multispectral Terrestrial Laser Scanning? A Case Study with Norway Spruce Seedlings. Frontiers in plant science, 9, 299. https://doi.org/10.3389/fpls.2018.00299

Kankare, V., Holopainen, M., Vastaranta, M., Puttonen, E., Yu, X., Hyyppä, J., Vaaja, M., Hyyppä, H., Alho, P., 2013. Individual tree biomass estimation using terrestrial laser scanning. ISPRS Journal of Photogrammetry and Remote Sensing, 75, 64-75. http://dx.doi.org/10.1016/j.isprsjprs.2012.10.003

Kankare, V., Liang, X., Vastaranta, M., Yu, X., Holopainen, M. & Hyyppä, J. 2015. Diameter distribution estimation with laser scanning based multisource single tree inventory. ISPRS Journal of Photogrammetry and Remote Sensing 108, 161–171. http://dx.doi.org/10.1016/j.isprsjprs.2015.07.007

Kankare, V., Joensuu, M., Vauhkonen, J., Holopainen, M., Tanhuanpää, T., Vastaranta, M., Hyyppä, J., Hyyppä, H., Alho, P., Rikala, J., Sipi, M., 2014. Estimation of the timber quality of Scots pine with terrestrial laser scanning. Forests, 5(8), 1879-1895. http://dx.doi.org/10.3390/f5081879

Kankare, V., Holopainen, M., Vastaranta, M., Liang, X., Yu, X., Kaartinen, H., Kukko, A., Hyyppä, J., 2017. Outlook for the Single-Tree-Level Forest Inventory in Nordic Countries. In: Ivan, I., Singleton, A., Horák, J., Inspektor, T. (Eds.), The Rise of Big Spatial Data. Lecture Notes in Geoinformation and Cartography. Springer, Cham, pp. 183–195. http://dx.doi.org/10.1007/978-3-319-45123-7_14

Koreň, M., Mokroš, M., Bucha, T., 2017. Accuracy of tree diameter estimation from terrestrial laser scanning by circle-fitting methods. International Journal of Applied Earth Observation and Geoinformation, 63, 122-128. https://doi.org/10.1016/j.jag.2017.07.015

Krankina, O.N., Harmon, M.E., 1995. Dynamics of the dead wood carbon pool in northwestern Russian boreal forests. Water, Air, and Soil Pollution, 82(1-2), 227-238. http://dx.doi.org/10.1007/BF01182836

Kukko, A., Kaartinen, H., Hyyppä, J., Chen, Y., 2012. Multiplatform mobile laser scanning: Usability and performance. Sensors 12(9), 11712–11733. http://dx.doi.org/10.3390/s120911712

Laasasenaho, J., 1982. Taper curve and volume function for pine, spruce and birch. Publications of Forest Research Institute in Finland. Communicationes Instituti Forestalis Fenniae, 108.

Liang, X., Hyyppä, J., 2013. Automatic stem mapping by merging several terrestrial laser scans at the feature and decision levels. Sensors, 13(2), 1614-1634. http://dx.doi.org/10.3390/s130201614

Liang, X., Litkey, P., Hyyppä, J., Kaartinen, H., Vastaranta, M., Holopainen, M., 2012. Automatic stem mapping using single-scan terrestrial laser scanning. IEEE Transactions on Geoscience and Remote Sensing 50(2), 661–670. http://dx.doi.org/10.1109/TGRS.2011.2161613

Liang, X., Kankare, V., Yu, X., Hyyppä, J., Holopainen, M., 2014a. Automated stem curve measurement using terrestrial laser scanning. IEEE Transactions on Geoscience and Remote Sensing 52, 1739–1748. https://doi.org/10.1109/TGRS.2013.2253783

Liang, X., Hyyppä, J., Kukko, A., Kaartinen, H., Jaakkola, A., Yu, X. 2014b. The use of a mobile laser scanning system for mapping large forest plots. IEEE Geoscience and Remote Sensing Letters 11(9), 1504-1508. https://doi.org/10.1109/LGRS.2013.2297418

Liang, X., Kankare, V., Hyyppä, J., Wang, Y., Kukko, A., Haggrén, H., Yu, X., Kaartinen, H., Jaakkola, A., Guang, F., Holopainen, M., Vastaranta, M., 2016. Terrestrial laser scanning in forest inventories. ISPRS Journal of Photogrammetry and Remote Sensing 115, 63–77. http://dx.doi.org/10.1016/j.isprsjprs.2016.01.006

Liang, X., Hyyppä, J., Kaartinen, H., Lehtomäki, M., Pyörälä, J., Pfeifer, N., Holopainen, M., Brolly, G., Francesco, P., Hackenberg, J., Huang, H., 2018. International benchmarking of terrestrial laser scanning approaches for forest inventories. ISPRS Journal of Photogrammetry and Remote Sensing, 144, 137-179.http://dx.doi.org/10.1016/j.isprsjprs.2018.06.021

Lindberg, E., Hollaus, M., Mücke, W., Fransson, J. E., Pfeifer, N., 2013. Detection of lying tree stems from airborne laser scanning data using a line template matching algorithm. ISPRS Annals of Photogrammetry, Remote Sensing and Spatial Information Sciences 5, 169-174. http://dx.doi.org/10.5194/isprsannals-II-5-W2-169-2013

Maas, H., Bienert, A., Schieller, S., Keane, E., 2008. Automatic forest inventory parameter determination from terrestrial laser scanner data. International Journal of Remote Sensing 29(5), 1579–1593. http://dx.doi.org/10.1080/01431160701736406

Marchi, N., Pirotti, F., Lingua, E., 2018. Airborne and Terrestrial Laser Scanning Data for the Assessment of Standing and Lying Deadwood: Current Situation and New Perspectives. Remote Sensing, 10(9), 1356. http://dx.doi.org/10.3390/rs10091356

Newnham, G.J., Armston, J.D., Calders, K., Disney, M.I., Lovell, J.L., Schaaf, C.B., Strahler, A.H., Danson, F.M., 2015. Terrestrial laser scanning for plot-scale forest measurement. Current Forestry Reports, 1(4), 239-251. http://dx.doi.org/10.1007/s40725-015-0025-5

Nyström, M., Holmgren, J., Fransson, J.E.S., Olsson, H., 2014. Detection of windthrown trees using airborne laser scanning. International Journal of Applied Earth Observation and Geoinformation 30, 21–29. http://dx.doi.org/10.1016/j.jag.2014.01.012

Olofsson, K., Holmgren, J., 2016. Single tree stem profile detection using terrestrial laser scanner data, flatness saliency features and curvature properties. Forests, 7(9), 207. http://dx.doi.org/10.3390/f7090207

Pasher, J., King, D.J., 2009. Mapping dead wood distribution in a temperate hardwood forest using high resolution airborne imagery. Forest Ecology and Management, 258(7), 1536-1548. http://dx.doi.org/10.1016/j.foreco.2009.07.009

Pesonen, A., Maltamo, M., Eerikäinen, K., Packalèn, P., 2008. Airborne laser scanning-based prediction of coarse woody debris volumes in a conservation area. Forest Ecology and Management, 255(8-9), 3288-3296. http://dx.doi.org/10.1016/j.foreco.2008.02.017

Polewski, P., Yao, W., Heurich, M., Krzystek, P., Stilla, U., 2017. A voting-based statistical cylinder detection framework applied to fallen tree mapping in terrestrial laser scanning point clouds. ISPRS Journal of Photogrammetry and Remote Sensing, 129,.118-130. https://doi.org/10.1016/j.isprsjprs.2017.04.023

Putman, E.B., Popescu, S.C., 2018. Automated Estimation of Standing Dead Tree Volume Using Voxelized Terrestrial Lidar Data. IEEE Transactions on Geoscience and Remote Sensing, (99). http://dx.doi.org/10.1109/TGRS.2018.2839088

Pyörälä, J., Kankare, V., Vastaranta, M., Rikala, J., Holopainen, M., Sipi, M., Hyyppä, J., Uusitalo, J., 2018. Comparison of terrestrial laser scanning and X-ray scanning in measuring Scots pine (Pinus sylvestris L.) branch structure. Scandinavian Journal of Forest Research, 33(3), 291-298. https://doi.org/10.1080/02827581.2017.1355409

Raumonen, P., Casella, E., Calders, K., Murphy, S., Åkerblom, M., Kaasalainen, M., 2015. Massive-scale tree modelling from TLS data. ISPRS Annals of the Photogrammetry, Remote Sensing and Spatial Information Sciences 2(3), 189–196. http://dx.doi.org/10.5194/isprsannals-II-3-W4-189-2015

Russell, M.B., Fraver, S., Aakala, T., Gove, J.H., Woodall, C.W., D'Amato, A.W., Ducey, M.J., 2015. Quantifying carbon stores and decomposition in dead wood: A review. Forest Ecology and Management, 350, 107-128. http://dx.doi.org/10.1016/j.foreco.2015.04.033

Saarinen, N., Kankare, V., Vastaranta, M., Luoma, V., Pyörälä, J., Tanhuanpää, T., Liang, X., Kaartinen, H., Kukko, A., Jaakkola, A., Yu, X., Holopainen, M., Hyyppä, J., 2017. Feasibility of Terrestrial laser scanning for collecting stem volume information from single trees. ISPRS Journal of Photogrammetry and Remote Sensing 123, 140–158. http://dx.doi.org/10.1016/j.isprsjprs.2016.11.012

Seidel, D., Albert, K., Ammer, C., Fehrmann, L., Kleinn, C., 2013. Using terrestrial laser scanning to support biomass estimation in densely stocked young tree plantations. International journal of remote sensing, 34(24), 8699-8709. http://dx.doi.org/10.1080/01431161.2013.848308

Siitonen, J., 2001. Forest management, coarse woody debris and saproxylic organisms: Fennoscandian boreal forests as an example. Ecological Bulletins 49, 11–41.

Similä, M., Kouki, J., Martikainen, P., 2003. Saproxylic beetles in managed and seminatural Scots pine forests: quality of dead wood matters. Forest Ecology and Management, 174(1-3), 365-381. http://dx.doi.org/10.1016/S0378-1127(02)00061-0

Söderström, L., 1988. Sequence of bryophytes and lichens in relation to substrate variables of decaying coniferous wood in northern Sweden. Nordic Journal of Botany, 8(1), 89-97. http://dx.doi.org/10.1111/j.1756-1051.1988.tb01709.x

Stovall, A.E., Vorster, A.G., Anderson, R.S., Evangelista, P.H., Shugart, H.H., 2017. Non-destructive aboveground biomass estimation of coniferous trees using terrestrial LiDAR. Remote Sensing of Environment, 200, 31-42. http://dx.doi.org/10.1016/j.rse.2017.08.013

Sun, Y., Liang, X., Liang, Z., Welham, C., Li, W., 2016. Deriving merchantable volume in poplar through a localized tapering function from non-destructive terrestrial laser scanning. Forests, 7(4), 87. http://dx.doi.org/10.3390/f7040087

Tanhuanpää, T., Kankare, V., Vastaranta, M., Saarinen, N., Holopainen, M. 2015. Monitoring downed coarse woody debris through appearance of canopy gaps in urban boreal forests with bitemporal ALS data. Urban Forestry & Urban Greening 14 (4), 835–843. http://dx.doi.org/10.1016/j.ufug.2015.08.005

Tikkanen, O.P., Martikainen, P., Hyvärinen, E., Junninen, K., Kouki, J., 2006. Red-listed boreal forest species of Finland: associations with forest structure, tree species, and decaying wood. In Annales Zoologici Fennici (373-383). Finnish Zoological and Botanical Publishing Board.

Finnish Forest Research Institute, 2009. Valtakunnan metsien 11. inventointi (VMI11) maastotyön ohjeet 2009 Koko Suomi, 2. painos. (In Finnish).

White, J.C., Coops, N.C., Wulder, M.A., Vastaranta, M., Hilker, T., Tompalski, P., 2016. Remote sensing technologies for enhancing forest inventories: A review. Canadian Journal of Remote Sensing, 42(5), 619-641. https://doi.org/10.1080/07038992.2016.1207484

Wilkes, P., Lau, A., Disney, M., Calders, K., Burt, A., de Tanago, J.G., Bartholomeus, H., Brede, B., Herold, M., 2017. Data acquisition considerations for terrestrial laser scanning of forest plots. Remote Sensing of Environment, 196, 140-153. http://dx.doi.org/10.1016/j.rse.2017.04.030

Yu, X., Hyyppä, J., Karjalainen, M., Nurminen, K., Karila, K., Vastaranta, M., Kankare, V., Kaartinen, H., Holopainen, M., Honkavaara, E., Kukko, A., Jaakkola, A., Liang, X., Wang, Y., Hyyppä, H., Katoh, M., 2015. Comparison of Laser and Stereo Optical, SAR and InSAR Point Clouds from Air- and Space-Borne Sources in the Retrieval of Forest Inventory Attributes. Remote Sensing 2015(7), 15933–15954. http://dx.doi.org/10.3390/rs71215809